RAA 2018 Vol. **18** No. **12**, 148(10pp) doi: 10.1088/1674–4527/18/12/148

http://www.raa-journal.org *http://iopscience.iop.org/raa*

***R**esearch in*
***A**stronomy and*
***A**strophysics*

A report on Type II X-ray bursts from SMC X-1

Binay Rai[1], Pragati Pradhan[2,3] and Bikash Chandra Paul[1]

[1] Dept. of Physics, North Bengal University, Darjeeling, West Bengal, 734013, India; *binayrai21@gmail.com*
[2] Department of Astronomy and Astrophysics, Pennsylvania State University, Pennsylvania, 16802, USA
[3] St. Joseph's College, Darjeeling-734104, West Bengal, India

Received 2018 March 20; accepted 2018 May 28

Abstract We study *RXTE* PCA data for the high mass X-ray binary source SMC X-1 between 2003–10 and 2003–12 when the source was in its high states. The source is found to be frequently bursting which can be seen as flares in lightcurves that occur at a rate of one every 800 s, with an average of 4–5 Type II X-ray bursts per hour. We note that typically a burst was short, lasting for a few tens of seconds in addition to a few long bursts spanning more than a hundred seconds that were also observed. The flares apparently occupied 2.5% of the total observing time of 225.5 ks. We note a total of 272 flares with mean FWHM of the flare ∼21 s. The rms variability and aperiodic variability are independent of flares. As observed, the pulse profiles of the lightcurves do not change their shape, implying that there is no change in the geometry of an accretion disk due to a burst. The hardness ratio and rms variability of lightcurves exhibit no correlation with the flares. The flare fraction shows a positive correlation with the peak-to-peak ratio of the primary and secondary peaks of the pulse profile. The observed hardening or softening of the spectrum cannot be correlated with the flaring rate but may be due to the interstellar absorption of X-rays as evident from the change in hydrogen column density ($n_{\rm H}$). It is found that the luminosity of the source increases with the flaring rate. Considering that the viscous timescale is equal to the mean recurrence time of flares, we fixed the viscosity parameter $\alpha \sim 0.16$.

Key words: accretion — accretion discs — pulsar: individual (SMC X-1) — stars: neutron — X-rays: binaries — X-ray: burst

1 INTRODUCTION

SMC X-1 is a high mass X-ray binary (HMXB) system in the Small Magellanic Cloud (SMC). A Type II X-ray burst from the source was discovered by Angelini et al. (1991) along with aperiodic variability of 0.01 Hz. It was discovered while comparing the burst with MXB 1730–355, which is known as a "Rapid Burster" (Lewin et al. 1976). The burst is considered to be due to viscous instability in the accretion disk characterised by a sharp rise and decay in the count rate of the lightcurve, with recurrence time ranging from ∼10 s to 1 h.

It may be pointed out here that a Type I X-ray burst (Lewin & Joss 1983) arises from a thermonuclear origin and displays a sharp rise and exponential decay in the intensity observed in the lightcurve along with a recurrence time of hours or days. The spectrum of a Type I burst is consistent with that of a blackbody followed by spectral softening in the burst decay. It was observed that in a "Rapid Burster" the average fluxes emitted in Type II X-ray bursts were 120 times larger than the average fluxes emitted in Type I X-ray bursts (Hoffman et al. 1978). The observed ratio of time-averaged persistent flux to time-averaged Type I X-ray burst flux lies between 10 and 10^3 (Lewin et al. 1993).

SMC X-1 is an HMXB system with a neutron star (Price et al. 1971) and the B0 supergiant SK 160 with mass $\sim 17.2\,M_{\odot}$ having an orbital period of ~ 3.9 days (Schreier et al. 1972). The X-ray source is eclipsed by the companion for 0.6 days. The source is found to have a regular spin up state $\sim 3.279 \times 10^{-11}$ Hz s^{-1} (Davison 1977; Wojdowski et al. 2000) with no spin down state as has been recorded in the source. The source is observed to have an orbital decay rate of $\sim 3.4 \times 10^{-6}$ yr^{-1}

(Levine et al. 1993; Wojdowski et al. 2000). It has been reported that SMC X-1 shows an aperiodic variation of $\sim (55 - 60)$ d due to obstruction of X-rays coming from the source by its tilted precessing accretion disk (Wojdowski et al. 2000). It is also regarded as an "intermediate-stage source" (Moon et al. 2003) between low-mass X-ray binaries (LMXBs) and X-ray pulsars along with some interesting intermediate-stage sources having a magnetic field from 10^8 to 10^{11} G and which undergoes either Type I or II X-ray bursts, or both, and may or may not have coherent pulsation. Examples of these types of sources are "the Bursting Pulsar" GRO J1744–28 (Fishman et al. 1995) which shows Type II characteristic bursts along with coherent pulsation, "the Rapid Burster" MXB 1730–355 (Lewin et al. 1976) undergoing both Type I and Type II X-ray bursts and "the Accreting Milli-second pulsar" SAX J1808.4–3658 (in in 't Zand et al. 1998) which undergoes Type I X-ray bursts with coherent pulsation.

SMC X-1 and GRO J1744–28 have some properties in common, namely both of them undergo Type II bursts with coherent pulsation (Li & van den Heuvel 1997). Their spin periods are also very small; for SMC X-1 it is ~ 0.71 s and that for GRO J1744-28 is ~ 0.47 s. They have steady spin up in their spin with the measured magnetic field value $\sim 10^{11}$ G (Bildsten & Brown 1997) and luminosity below an Eddington limit. However in the case of GRO 1744–28, bursts occur at a higher rate than SMC X-1, although they also differ in burst pattern. The analysis of *Rossi X-ray Timing Explorer* (*RXTE*) Proportional Counter Array (PCA) data targeting SMC X-1 by Moon et al. (2003) found that the flare occupies 3% of the total observing time and is spread over different orbital phases, and is strongly correlated with variability in the lightcurve. The flare fraction is found to increase with the peak to peak ratio of the pulse profile. The properties of SMC X-1 do not differ very much during the flaring period from those of the normal state. Here, we study detailed properties of Type II X-ray bursts from SMC X-1 by making use of *RXTE* PCA data between 2003–10 and 2003–12. The organization of the paper is as follows: In Section 2 we discuss the data reduction to analyze the source. In Section 3 study of lightcurves with flares is presented. Section 4 is concerned with study of the pulse profile, hardness ratio and spectrum of the source. Section 5 deals with study of the correlation between bursts with different parameters and also investigates the relation of luminosity with flaring rate. Finally a discussion is given in Section 6.

2 DATA SELECTION AND REDUCTION

To investigate the source SMC X-1, we used *RXTE* PCA data. PCA has an array of five proportional counter units (PCUs), namely PCU 0, PCU 1, PCU 2, PCU 3 and PCU 4 (Jahoda et al. 2006). PCU 0 suffered propane loss in the year 2000. PCU 3 and PCU 4 were regularly rested to avoid breakdown. Out of the above mentioned counter units, data from PCU 2 will be employed here for analysis as it was the only PCU unit that did not suffer any breakdown and was operating all the time. PCU 2 is the best calibrated counter unit as verified by fitting the Crab spectrum simply with a power law (PL).

The data reduction was done using HEASOFT ver 6.11. For spectral analysis, standard 2 mode of *RXTE* PCA data was used which has 129 channels and default binning of 16 s. The data from only the top Xe-layer of PCU 2 were considered. The response matrix for the top layer has been obtained using *FTOOL PCARSP*. The background spectra were extracted using the tool *RUNPCABACKEST* taking a bright source background model. The source spectra were then produced by subtracting these background spectra with the total spectra in *XSPEC*. Here the energy range for a spectrum under consideration lies in the range 3–18 keV. We have not considered data above 18 keV as the spectrum in that case is dominated by background and good fitting may not be possible. A systematic error of 2% was added to all spectra.

Timing analysis was carried out using the *GOODXENON* mode of *RXTE* PCA data. The lightcurves were extracted from the *GOODXENON* data using the mission specific tool *SEEXTRCT* for the whole available energy range and all layers of PCU 2 with background correction. Background correction was applied by subtracting the background lightcurve from the total lightcurve using *lcmath*. The background lightcurve was extracted using the background model for the bright source. The reference frame of photon arrival time was transformed to the barycentre with the help of *FTOOL FAXBARY* using JPL DE400 ephemeris. The set of data where the elevation of the telescope was $<10^\circ$ and 30 min after the passage from the South Atlantic Anamoly (SAA) has been considered in this paper for data reduction and analysis.

3 LIGHTCURVES AND FLARES

For our analysis, in addition to flares, we searched for all *RXTE* PCA data available for SMC X-1 between 2003–

10 and 2003–12. The data we have considered lie in two high states, h1 and h2, as observed in the *RXTE* ASM lightcurve of the source, as shown in Figure 1. The technique used by Moon et al. (2003) to search for flares is followed in this work. All the photon counts which were 3σ above the mean are considered to be a flare in a lightcurve. The data were divided into 110 data segments, with each segment having duration $\sim$ 2050 s. Hence, we have 110 lightcurves, each of which has been plotted and analyzed.

The time spent by a burst varies from burst to burst where some of them last for a few tens of seconds to much more than that. To determine the duration of a burst, we fit each flare with a Gaussian model to obtain the width 'w' of the flare. Consequently the full width at half maximum (FWHM) of a flare may be obtained by using the relation FWHM $= 2.35482w$, which we take as the duration of a burst. The reduced χ^2 of the fitting varies from 2.3 to 3.56. We began with the lightcurves that have a 4 s time resolution. We found 272 such cases of flares with mean FWHM of $\sim$ 21 s and mean standard deviation of $\sim$ 8 s. Therefore out of 225.5 ks, we note 5.7 ks as the time of flaring. Thus it is clear that the source is flare active for $\sim$2.5% of the total time which is close to the value reported earlier by Moon et al. (2003). The left panel of Figure 2 shows the lightcurves for four different observations, with a time resolution of 4 s and the corresponding normalised power spectra on the right. It is observed from the plot that the recurrence time between flares varies from a few hundred to a few thousand. The average value of recurrence time between flares from the above analysis is $\sim$ 800 s. The number of flares, width of flares and recurrence time are found to be the same for the lightcurves having time resolutions of 2 s, 6 s and 8 s.

For power spectra we use data with the time resolution of 0.075 s and we plot them using the XRONOS tool *POWSPEC* with normalization $= -2$. The value of normalization gives us the white noise normalised power spectra with their integral yields fractional root mean square (rms) variability. The power spectra corresponding to four lightcurves (left Fig. 2) are displayed in the right panel of Figure 2. The rms variabilities of the four lightcurves obtained from the power spectra are estimated to be (a) 30.86%, (b) 31.2%, (c) 31.2% and (d) 30.6%. Thus during all four observations the source is found to show the same variability, i.e. the source was equally variable.

Along with the coherent peak at frequency equal to the frequency of rotation of the pulsar ($\sim$ 1.41 Hz), peaks are also observed in frequencies which are integral multiples of the rotational frequency. Due to presence of aperiodic components some rise in power spectra is seen at low frequency range. For the power spectrum (d) it is noted that as we go to the low frequency region (from 1 to 0.005 Hz), power rises moderately and at $\sim$ 0.019 Hz a broad peak exists. A similar rise is seen in the right of Figure 2(c) at the same frequency as the flat top.

It is observed that during some flares the count rate reached up to many times the mean value, while, in some cases, flares were found to last for more than hundreds of seconds (Fig. 3). Generally, the bursts are single peaked (Fig. 2), however large bursts were found to have multiple peaks before they finally decayed to the mean value as shown in Figure 3. The left panel of Figure 3 shows a lightcurve with a flare of duration $\sim$ 50 s consisting of two sharp peaks. The first peak arises because of a sharp increase in the count rate, reaching $\sim$1350 s^{-1} then sharply falls to $\sim$510 s^{-1}, followed once again by an increase in count rate giving a second peak of $\sim$1320 s^{-1} which falls rapidly below 500 s^{-1}. The situation is such that one burst is followed by another one immediately. However, the flare shown in the right panel of Figure 3 is long, $\sim$300 s, and has multiple peaks; the highest peak has a count rate of $\sim$1000 s^{-1}, signalling the instability lasts for a long time and comes to a normal stable state with slow rise and decay in intensity with multiple peaks. The burst per hour per observation for the first high state (h1) as shown in Figure 1 is $\sim$5 h^{-1} and for the second (h2) we note $\sim$4 h^{-1}. However, for the complete observation, the average number of bursts per hour was $\sim$5 and the average time between two bursts may be set as $\sim$800 s.

4 PULSE PROFILE, HARDNESS RATIO AND ENERGY SPECTRA

The binary orbit of SMC X-1 is found to be nearly circular (Levine et al. 1993; Wojdowski et al. 2000; Raichur & Paul 2010). As the neutron star moves in its circular binary orbit there are delays in the pulse arrival time because of orbital modulation, i.e. when the neutron star is close to an observer, the pulse will arrive sooner than when the neutron star is away from the observer. In order to get a correct pulse profile, the arrival time of a pulse must be corrected so that we get an arrival time which also includes the effect of orbital modulation. If t'_n and t_n are the times of emission and arrival respectively then

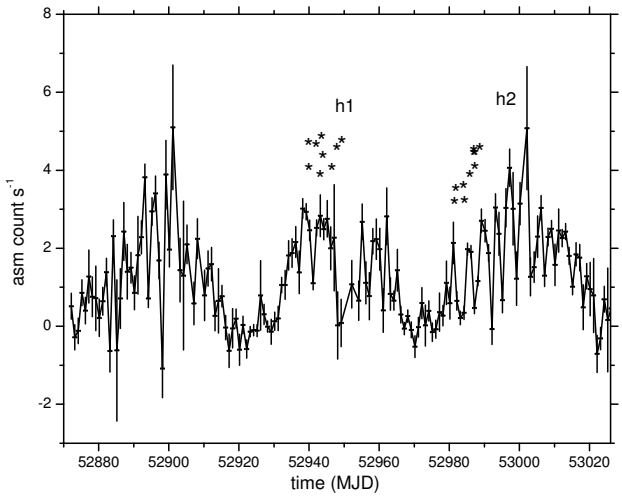

Fig. 1 A segment of the *RXTE* ASM lightcurve of SMC X-1 with rebinning of 1 day. The star symbols indicate the dates of the observations. Our observations of the source occurred during two high states as indicated by h1 and h2.

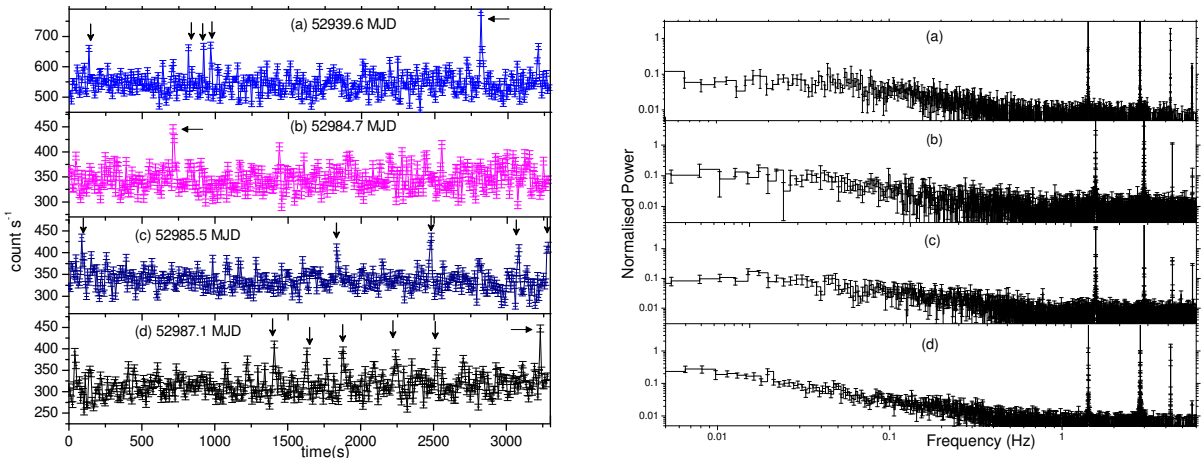

Fig. 2 The left panel of the figure displays the lightcurves of four different observations as indicated by lower case letters (a), (b), (c) and (d) with the date in MJD. The right panel shows their corresponding power spectra. The flares are indicated by *arrows* in the lightcurves. The power in power density spectra is expressed in the unit of (rms)^2 Hz^{-1}.

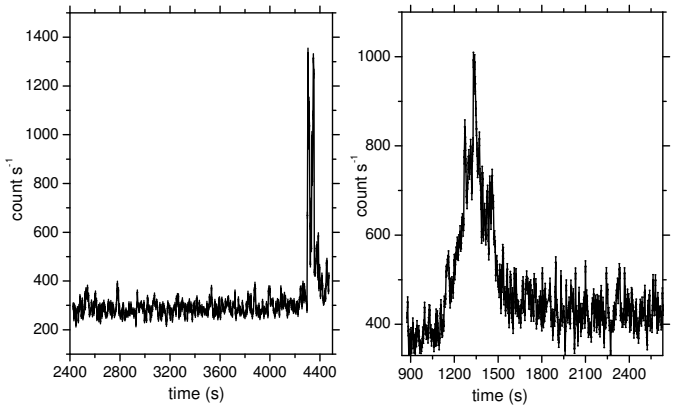

Fig. 3 Two large bursts observed in SMC X-1. The Obs.Id for the observation is 80078-01-01-04. The left panel shows the burst where the count rate rises up to ∼4 times above the mean value and in the right one the burst lasts for ∼300 s. Both of the bursts have multiple peaks.

they are related to each other and to the orbit of the neutron star through $f_{\rm orb}(t'_n)$ (Deeter et al. 1981) as

$$t'_n = t_0 + nP_s + \frac{1}{2}n^2\dot{P}_sP_s\,,$$
$$t_n = t'_n + f_{\rm orb}(t'_n)\,,$$

where P_s and $\dot{P}_s$ are respectively the spin period and time derivative of the spin period for the neutron star. For a circular orbit, $f_{\rm orb}(t'_n)$ takes the form

$$f_{\rm orb} = a_x \sin i \cos l_n\,,$$
$$l_n = 2\pi(t'_n - E)/P_{\rm orb} + \pi/2\,,$$

where l_n is the mean orbital longitude at time t'_n, E is the epoch when the mean orbital longitude is equal to $\pi/2$ and $a_x \sin i$ is the projected semi-major axis with 'i' being the angle of inclination between the line of sight and orbital angular momentum vector.

We have used the value of epochs and other orbital parameters from Raichur & Paul (2010) for the orbital correction. The orbital corrected pulse profiles are shown in Figure 4. The pulse fraction of (a) and (d) is 20% whereas for (b) and (c) it is 30%. All the pulse profiles have their secondary peak at a phase ∼0.78 and primary at ∼0.28. The secondary peaks of all four lightcurves coincide with each other. Except for the change in pulse fraction, there is no significant change in the pulse profiles.

The hardness ratios for the four observations were obtained by dividing the 7–16 keV energy X-ray photon count rate by the 3–7 keV energy X-ray photons count rate. The average hardness ratios for the four lightcurves are 0.9 ± 0.03, 0.897 ± 0.035, 0.8563 ± 0.031 and 0.837 ± 0.031 respectively, as displayed in Figure 5(a), 5(b), 5(c) and 5(d). The average hardness ratios for the four observations do not vary significantly. Also there is no noticeable change in hardness ratio in any of the four lightcurves during a burst. Therefore, the hardness ratio may not be correlated with flares from the source. We can check this invariance in the hardness ratio by studying the energy spectra of the source.

The energy spectra for four observations are shown in Figure 6. The models we have used for fitting these spectra are PHABS to estimate the photoelectric absorption of the photon by an interstellar medium, POWERLAW, HIGHECUT for the non-thermal emission of the source and GAUSSIAN for the iron line. The Gaussian peak for an iron line is fixed at 6.7 keV. The best fit parameters of the fit are shown in Table 1. For all observations, the PL indices are nearly the same; for the first three it is ∼1, as displayed in Figure 6(a), 6(b) and 6(c) whereas it is ∼1.1 for Figure 6(d). None of the best fit parameters changed significantly for the four spectra. Considering the distance of SMC X-1 from the observing point at 65 kpc (Keller & Wood 2006; Naik & Paul 2004) the luminosity of the source is measured, which for the four observations are are 6.787×10^{38}, 6.302×10^{38}, 6.211×10^{38} and 5.862×10^{38} erg s^{-1} respectively for Figure 6(a), 6(b) 6(c) and 6(d). The variation of the $n_{\rm H}$ value may be due to partial obscuration of the neutron star by the precessing accretion disk or X-ray eclipses. Another possibility for the variation may be an artifact of a simple POWERLAW model or the tails of the soft excess components affecting our result (Inam et al. 2010). The photoelectric absorption by interstellar matter is dominant in the lower energy range but as we cannot go below an energy of 3 keV due to the limitation of our instrument, it is not possible to constrain the $n_{\rm H}$ value precisely.

4.1 Variation of the Spectral Parameter with Orbital Phase and Flux

To study the variation of different spectral parameters over the binary orbit, the available spectra in the energy range 3–18 keV are fitted with the models discussed above, and the reduced χ^2 of the fitting lies between 1 and 2. We plotted the hydrogen column density ($n_{\rm H}$) and photon index with orbital phase. Spectral flux between the energy range 3–18 keV was also plotted with phase. From the left panel of Figure (7), we can see that there is no abrupt change in the photon index or $n_{\rm H}$ value with orbital phase. It is evident from Figure 7(c) that the flux lies between $0.992\pm0.001\times10^{-9}$ and $1.7326\pm0.001\times10^{-9}$. The maximum flux is at an orbital phase of 0.44 and the minimum at 0.16. The minimum of the $n_{\rm H}$ value is $1.01662 \times 10^{22}\,{\rm cm}^{-2}$ and it happens when the flux is maximum. As is evident from Figure 7(a), 7(c) and 7(d), the spectrum is a bit softer at phase 0.17 with the maximum value of the photon index, i.e. 1.16604 ± 0.3048, along with the maximum value of hydrogen density column 2.4156×10^{22}. The spectrum becomes harder with photon index 0.9574 ± 0.02 as the flux becomes maximum. From Figure 7(b) and 7(d) we can see there is no correlation of spectral softening or hardening with either phase or flux. The small hardening of the spectrum with minimum hydrogen density column may be because of the low absorption of hard X-ray by the interstellar medium, which also results in maximum flux observed

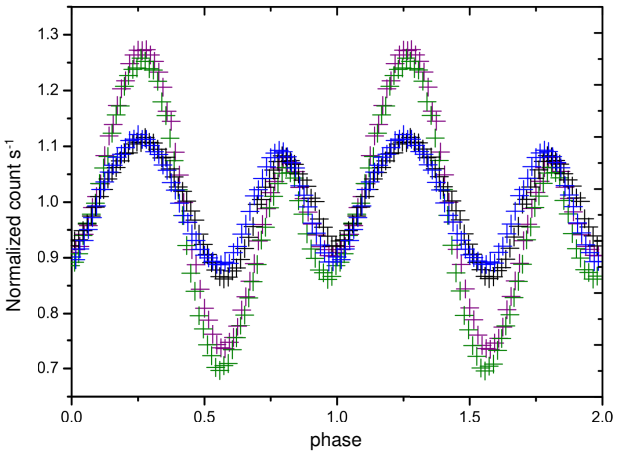

Fig. 4 Orbital corrected pulse profiles of the four lightcurves displayed in the left panel of Figs. 2(a), (b), (c) and (d) folded at ∼0.7 s; blue (a), purple (b), green (c) and black (d) .

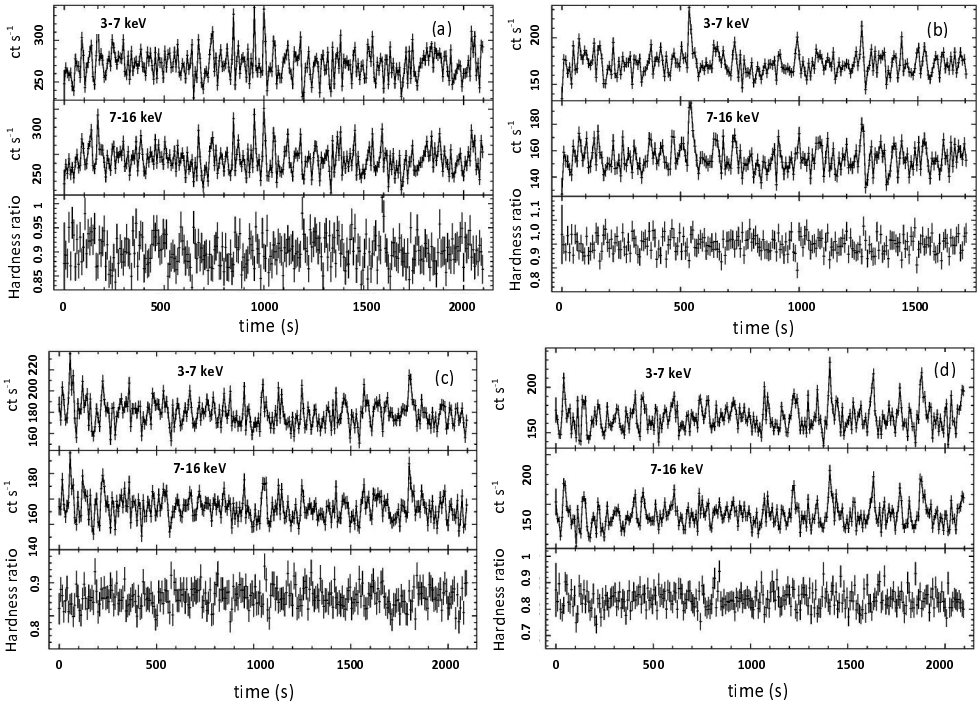

Fig. 5 Hardness ratio of four observations (a), (b), (c) and (d) obtained by dividing the X-ray photon count rate of 16 keV by 3-7 keV plotted with the time resolution of 8 s.

Table 1 The best-fit parameters of the fit. χ^2_ν is the reduced chi-square of the fit for 29° of freedom. $n_{\rm H}$ is the hydrogen column density of intervening interstellar matter. α is the PL index. $E_{\rm cutoff}$ and $E_{\rm fold}$ are the cutoff energy and e-folding energy of the model HIGHECUT expressed in keV respectively. The measured flux is for energy range 3–18 keV and in the unit 10^{-9} erg s^{-1} cm^{-2}.

Observation	a	b	c	d
$n_{\rm H}$	2.062± 1.023	1.014± 1.06	1.604± 1.043	1.968± 1.019
α	1.066±0.202	1.004±0.219	1.084±0.218	1.122±0.202
$E_{\rm fold}$	17.868±4.726	16.521±4.457	17.723±5.078	17.080±4.143
$E_{\rm cutoff}$	5.998±1.045	5.870±1.074	5.837±1.147	6.002±1.218
flux	1.345	1.247	1.229	1.160
χ^2_ν	1.682	1.375	1.890	1.563

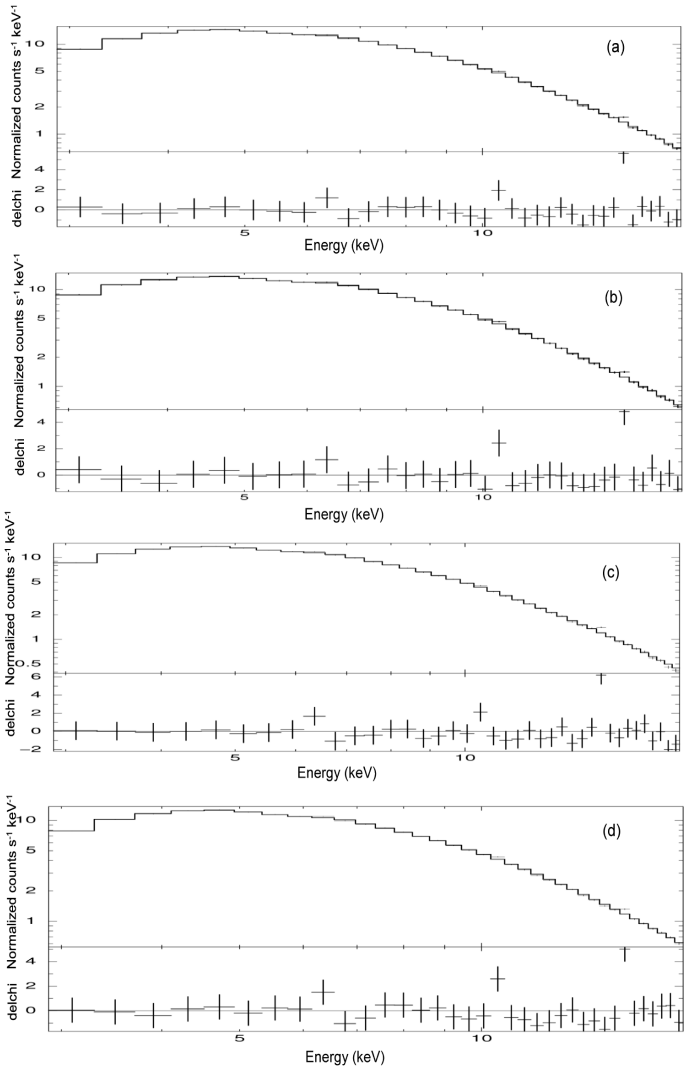

Fig. 6 Energy spectra (d) along with their best-fit spectra. The lower panel of each spectrum is the $\Delta\chi^2$ of the fit, which is the ratio of the difference of the observed data and the model value to the corresponding error.

at that phase. Similarly, the small softening of the spectrum may result from an increase in absorption of X-rays by the interstellar medium. The overall variation of the flux may be due to variation in the accretion rate of the neutron star.

5 CORRELATION OF THE FLARES WITH TIME, PHASE PEAK TO PEAK RATIO AND ORBITAL PHASE

The number of flares observed depends on the total observation time as shown in Figure 8(a). Thus it may be concluded that if the observation time is longer, greater numbers of flares may be observed. We did not find any correlation of the flare fraction with rms variability of the lightcurve of the source. The rms variability was found to lie between $\sim 30\% - 33\%$ with an average of $\sim 31\%$. To investigate the correlation of the flares with pulse profile peak-to-peak ratio, we divide the flare fraction of a particular observation by time so the flare fraction is now measured in $\%$ h^{-1} and plotted with the peak-to-peak ratio of secondary to primary peaks of the pulse profiles. The flare fraction per hour shows some correlation with the peak-to-peak ratio (Fig. 8b), as there is a relative increase in the flare fraction per hour. However it is evident from Figure 8(c) that no correlation of the flare fraction with orbital phase exists. The flare fraction/h is constant from $\sim$ 0.05 to $\sim$ 0.3 then starts decreasing except near 0.2 where a change is observed; it is noted that near 0.56 an increase in the flare fraction is also observed. This variation of flare fraction with orbital phase

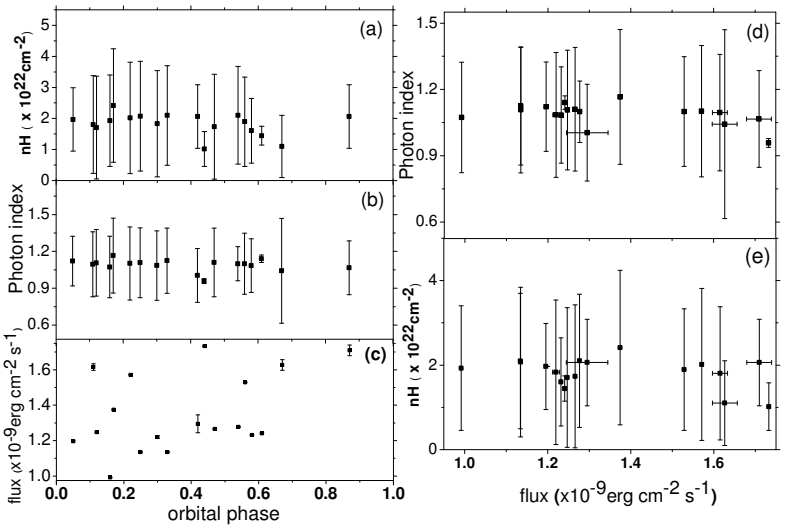

Fig. 7 The variations of $n_{\rm H}$, photon index of PL and flux are displayed in panels (a), (b) and (c) respectively, whereas panels (d) and (e) give the variation of photon index and $n_{\rm H}$ with flux respectively.

may be due to the varying accretion rate of the neutron star, which changes the number of bursts observed. To know whether flaring is the reason behind the change in photon index, which results in the softening or hardening of the spectrum, we plotted the photon index of the spectrum with respect to the flare fraction/h of different observations (Fig. 8f). As observed in Figure (8f), one cannot correlate the change in photon index with the change in flare fraction, however the spectrum looks harder when the flare fraction/h(%) is ~ 10. As there is no correlation of photon index with flare fraction, one can conclude that the hardening of the spectrum in this case may be due to a decrease in absorption by the interstellar medium, not due the increase in flaring rate.

The variation of spin period of the neutron star with luminosity of the source is depicted in Figure 8(d). The spin periods were obtained by using the timing tool EFSEARCH in orbitally corrected data obtained by following the method described in Section 4. The spin period in our observations lies between $\sim$0.7033 and $\sim$0.7057 with the luminosity ranging from 3.9×10^{38} to 7.8×10^{38} erg s^{-1}. The spin-up rate is found to be directly proportional to $PL_{38}^{3/2}$ where (P) is the spin of the neutron star and (L_{38}) is the luminosity of the source. As the spin up rate $\dot{P}$ is small, about $\sim 3.279 \times 10^{-11}$ Hz s^{-1} (Davison 1977; Wojdowski et al. 2000) and the two high states are separated by $\sim$50 d, there is negligible spin up. Hence the variation of the spin (P) with luminosity (L_{38}) is $PL_{38}^{3/2} =$ constant (Ghosh & Lamb 1979). In our case, we do not see such variation of spin for the source with its luminosity, which may be because of the fact that the data we have considered span a few months of observations of the source. It can be possible to find the relation between luminosity and spin, and also possibly the relation between spin-up rate, spin and luminosity with the help of long term study of the source. But in a source like SMC X-1, it is harder to study the spin-luminosity relation because of superorbital modulation of luminosity which causes the luminosity to vary in an aperiodic manner. The luminosity of the source increases with the increase in flares as evident from Figure 8(e), i.e. the luminosity of the source has a strong positive correlation with flares.

6 DISCUSSION

The source SMC X-1 emits Type II bursts with the mean recurrence time of $\sim$800 s and for 2.5% of the observed time the source was bursting. The Type II bursts are due to Lightman-Eardley (LE) instability, which develops in the viscous accretion disk. The average number of bursts per hour is found to be $\sim 4-5$. Thus SMC X-1 is an HMXB "bursting pulsar." We notice a large burst of very short duration and one with long duration with multiple peaks. However, the observed pulse profiles do not change their shape despite the fact that the different observations were carried out in different bursting states, signalling that the accretion disk geometry has not changed because of the burst. The peak-to-peak ratio of the spin-phase increases with the increase in flaring

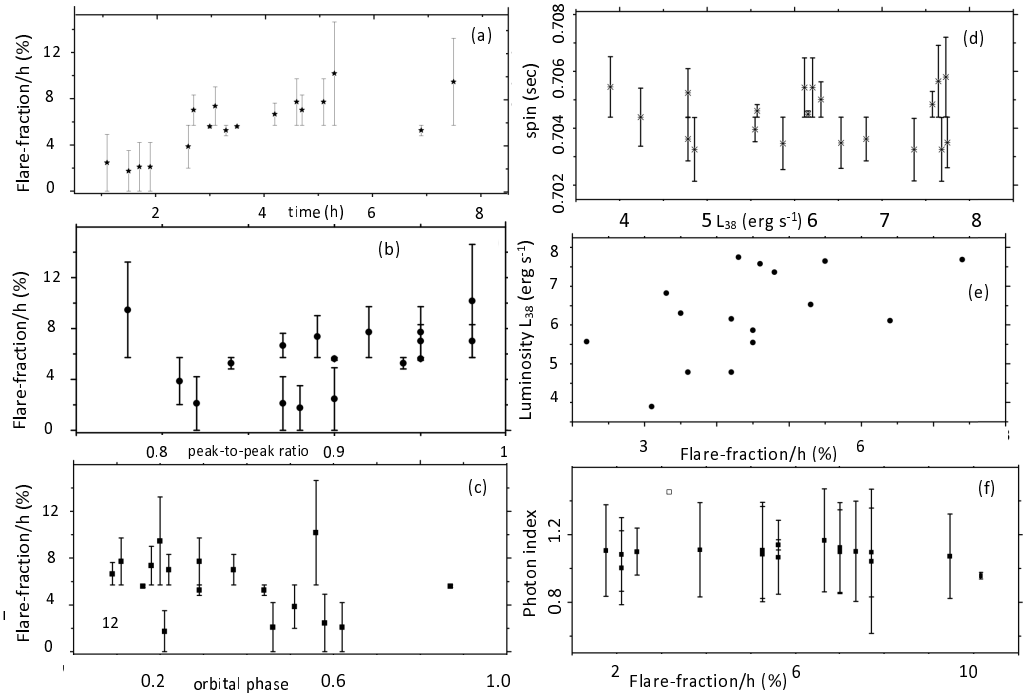

Fig. 8 The variation of flare fraction with the time of observation (a), with the pulse profile peak-to-peak ratio (b) and with the orbital phase (c). For (b) and (c), the average flare fraction, i.e. flare fraction per hour, is plotted against peak-to-peak ratio and orbital phase respectively. The variation of spin with luminosity is plotted in (d) and in (e) the variation of luminosity with flare fraction is shown. Panel (f) displays the variation in photon index of the spectrum with flare fraction per hour.

rate which may be due to the greater rate of accretion of matter at the cooler pole as compared to the hotter pole of the neutron star during bursts (Moon et al. 2003). We suspect that the increase in accretion rate above leads to the associated instability, so the increase in accretion rate may cause nearly equal accretion of matter at both the poles, resulting in nearly equal primary and secondary peaks as observed in the pulse profile. The luminosity of the source is found to increase with the increase in flaring rate as the conversion of matter into radiation takes place at a higher rate than during a normal state.

LE instability is seen when the radiation pressure becomes dominant and is a major contributor to the total pressure. The instability is followed by thermal and surface density instability. The global nature of the instability was investigated by Taam & Lin (1984) and Lasota & Pelat (1991) who found that the instability results in bursts which recur after a few seconds. This phenomenon was similar to the three outbursts observed in the lightcurve of GRO J1744–28 during 1996 (Cannizzo 1996), which had outbursts of ~ 10 s and recurrence times of $\sim$1000 s. According to Cannizzo, the fast timescale seen by Taam & Lin (1984) and Lasota & Pelat (1991) was because they set the viscosity parameter 'α' (Shakura & Sunyaev 1973) equal to one and considered the inner radius ($r_{\rm inner}$) of the accretion disk equal to the neutron star radius. ($R \sim$10 km). It has been pointed out that for outbursts to occur in GRO J1744–28, the accretion rate must exceed the critical value by a small amount at which the radiation pressure is comparable to the gas pressure. Taking a reasonable value of α (less than 1 and $r_{\rm inner}$ greater than R), the viscous timescale at the critical condition has been found to equal $t_{\nu,\rm crit} = 1200 r_8^{0.58} m^{0.79}$ s, where $r_8 = r_{\rm inner}/10^8$ cm, $m = M/M_\odot$ and M is the mass of the neutron star which is in good agreement with the recurrence time of the burst in GRO J1744-28 provided by $r_{\rm inner} = 10^{7.5}$ cm and $M = 1.4\,M_\odot$ (Cannizzo 1996), $t_{\nu,\rm crit} \sim$800 s. The burst from SMC X-1 is similar to that of GRO 1744–28 but we note that the post-flare dip is absent in the former. The absence of the dip in the former may be due to the slow accumulation of matter after the burst or because of the release of only a certain amount of accumulated matter during the burst so that after the burst intensity is found at the persistent level. Another possibility for there being no dip observed in the SMC X-1 after the burst may be due to the increase in accretion rate just after the burst.

There was no correlation between flare fraction/h, $n_{\rm H}$ and flux with the orbital phase. There is no evidence of a change in the nature of the spectrum because of flares. The small softening or hardening of the spectrum was not due to flares but may be due to varying interstellar absorption. The spectrum of the burst for SMC X-1 shows similar properties to GRO J1744–28 as there is no spectral softening, but it is also inconsistent with the associated blackbody, and the photon index is $\sim$1.2 and the high cutoff energy is 14 keV (Sazonov et al. 1996). We may conclude that the bursts in the two X-ray binaries are due to LE instability with a comparable magnetic field. Due to the presence of a low magnetic field, the transition region (between the radiation dominated and gas pressure dominated region) is located near the inner edge of the disk (Li & van den Heuvel 1997), therefore, the instability develops inside the disk which is not carried far and heats the surrounding matter because of increasing viscosity. The heated matter is then accreted onto the neutron star producing a burst. From Moon et al. (2003), in the transition region between the radiation dominant and pressure dominant regions, the viscous timescale is

$$\alpha = 216\dot{M}_{17}/t_{\rm visc}^{\frac{3}{2}},$$

where $\dot{M}_{17}$ is the accretion rate on the order of 10^{17} and $t_{\rm visc}$ is the viscous timescale. Taking the typical value of $\dot{M}_{17} = 20$ g ms^{-1} and $t_{\rm visc} = 800$ s, $\alpha \sim 0.16$. If the recurrence of the burst occurs on the same timescale as that of the viscous timescale then we can say $\alpha \sim 0.16$. The accumulation of a huge amount of matter during a short time may lead to large bursts in a short time. However, if accumulation of matter happens slowly it results in instability that develops in a large area for a long time over the disk, causing long bursts with multiple peaks.

The aperiodic variability of the power spectra can be a possible low frequency quasi-periodic oscillation (QPO) because of interaction of the magnetosphere of the pulsar with the inner edge of the accretion disk as observed in EXO 2030+375 and Cen X-3 or "peaked low frequency noise" seen in LMXRB's Sco X-1 and GX 17+2 (Angelini et al. 1991). Our observation suggests that the flaring activity of the pulsar bears no correlation with this aperiodic variability as seen in Figure 2, in which the aperiodic variability exists whether the number of flares increases or decreases. The rms variability of the lightcurves of the sources is observed to be independent of the flares, implying the source was varying equally all the time.

Acknowledgements This research has made use of data obtained through the High Energy Astrophysics Science Archive Research Center (HEASARC) Online Service, provided by NASA's Goddard Space Flight Center. BCP would like to acknowledge SERB-DST for the research grant EMR/2016/005734. The authors would like to thank the anonymous reviewer for his/her valuable comments and suggestions.

References

Angelini, L., Stella, L., & White, N. E. 1991, ApJ, 371, 332
Bildsten, L., & Brown, E. F. 1997, ApJ, 477, 897
Cannizzo, J. K. 1996, ApJ, 466, L31
Davison, P. J. N. 1977, MNRAS, 179, 15P
Deeter, J. E., Boynton, P. E., & Pravdo, S. H. 1981, ApJ, 247, 1003
Fishman, G. J., Kouveliotou, C., van Paradijs, J., et al. 1995, IAU Circ., 6272
Ghosh, P., & Lamb, F. K. 1979, ApJ, 234, 296
Hoffman, J. A., Marshall, H. L., & Lewin, W. H. G. 1978, Nature, 271, 630
in 't Zand, J. J. M., Heise, J., Muller, J. M., et al. 1998, A&A, 331, L25
Inam, S. Ç., Baykal, A., & Beklen, E. 2010, MNRAS, 403, 378
Jahoda, K., Markwardt, C. B., Radeva, Y., et al. 2006, ApJS, 163, 401
Keller, S. C., & Wood, P. R. 2006, ApJ, 642, 834
Lasota, J. P., & Pelat, D. 1991, A&A, 249, 574
Levine, A., Rappaport, S., Deeter, J. E., Boynton, P. E., & Nagase, F. 1993, ApJ, 410, 328
Lewin, W. H. G., Doty, J., Clark, G. W., et al. 1976, ApJ, 207, L95
Lewin, W. H. G., & Joss, P. C. 1983, in Accretion-Driven Stellar X-ray Sources, ed. W. H. G. Lewin & E. P. J. van den Heuvel, 41
Lewin, W. H. G., van Paradijs, J., & Taam, R. E. 1993, Space Sci. Rev., 62, 223
Li, X.-D., & van den Heuvel, E. P. J. 1997, A&A, 321, L25
Moon, D.-S., Eikenberry, S. S., & Wasserman, I. M. 2003, ApJ, 582, L91
Naik, S., & Paul, B. 2004, A&A, 418, 655
Price, R. E., Groves, D. J., Rodrigues, R. M., et al. 1971, ApJ, 168, L7
Raichur, H., & Paul, B. 2010, MNRAS, 401, 1532
Sazonov, S., Sunyaev, R., & Swank, J. 1996, IAU Circ., 6291
Schreier, E., Giacconi, R., Gursky, H., Kellogg, E., & Tananbaum, H. 1972, ApJ, 178, L71
Shakura, N. I., & Sunyaev, R. A. 1973, A&A, 24, 337
Taam, R. E., & Lin, D. N. C. 1984, ApJ, 287, 761
Wojdowski, P. S., Clark, G. W., & Kallman, T. R. 2000, ApJ, 541, 963